PATTERN EXTRACTION BY ADAPTIVE PROPAGATION OF A REGIONAL THRESHOLD[1]

Shriram Revankar and David B. Sher
Department of Computer Science
State University of New York
Buffalo, New York 14260

Keywords: pattern extraction, adaptive, threshold, evaluation, line images, echocardiogram.

Abstract

We describe a method for pattern extraction by adaptive propagation of a regional threshold to the rest of the image. In most images there is an easily thresholded region. We propagate the regional threshold to the entire image using a linear approximation of the image intensity gradients. This method is useful in the fields where the extraction of precise geometry of the binarized patterns is required, and in the fields where continuous thin lines are to be extracted.

1 Introduction

Thresholding is a popular way to segment an image of a binary scene. Conventionally, thresholding methods concentrate on pattern *detection* problem. The *extraction* problem is determination of the geometry of the foreground object in the image. In applications that need the geometry of the thresholded pattern to be directly proportional to the object geometry, the thresholding algorithms must address both the detection and the extraction problems. For example, in echocardiography cardiologists obtain the heart wall thickness, ventricular volume, etc. by direct measurement of the pattern extracted from a two dimensional echocardiograms [1]. Furthermore, in line images, it is often advantageous to extract a thin line pattern [2].

If the illumination of the scene is uniform and the object region is of uniform grey value, a properly selected global threshold can satisfactorily extract the pattern. In real images it is difficult to maintain uniform illumination. A large fraction of the real images of binary scenes such as printed or hand written text, ultrasound images of heart, etc. exhibit nonuniform reflectance, and require pattern extraction for higher level processing.

To account for the variations in illumination and reflectance, several researchers have proposed adaptive methods, where the threshold is a function of image intensities in the neighborhood of a pixel [3, 4], and the position of the pixel to be thresholded [5]. Adaptive techniques are usually domain dependent, *i.e.* they

[1]This research is supported by a grant (#91-050G) from the New York state affiliate of the American Heart Association

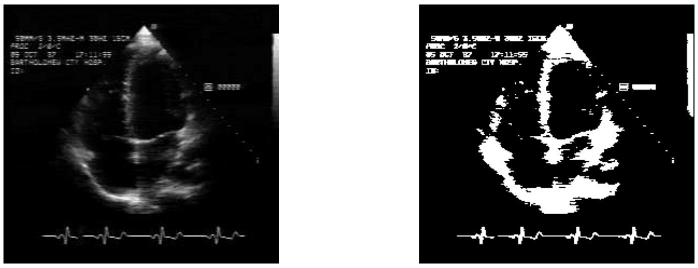

Figure 1: A typical two dimensional echocardiogram, and its thresholded pattern generated by the optimal global threshold,t=27.

account for the variations that could occur in a particular domain. For example, Wolfe [6] and Ogawa *et al.*[7] assumed that in text images, width of a limb does not exceed a known limit. In this paper we develop an adaptive threshold propagation method for a domain of images with line patterns and elongated patterns.

Several early thresholding methods have been discussed by Weszka [8], and Sahoo *et al*[9] provide an excellent survey of many recent thresholding methods. They have also suggested two methods to evaluate and compare thresholding methods, namely, *Uniformity measure* and *Shape measure*. We will briefly study these two evaluation methods, and try to highlight the need for a thresholding method for *pattern extraction* in contrast to *pattern detection*. In Figure 1, we show a typical four chamber, long axis echocardiogram image, and its binary pattern generated by the optimal global threshold. The threshold was manually selected by observing the thickness of the detected wall pattern. Though the threshold is inaccurate at certain locations, it does preserve the shape and size of the heart wall pattern for the most part. We study the threshold evaluation methods with reference to this image and the threshold.

1.1 Uniformity criterion

Sahoo *et al*[9] define the uniformity measure as follows:

$$U(t) = 1 - \frac{\sigma_1^2(t) + \sigma_2^2(t)}{C} \tag{1}$$

where $\sigma_1^2(t)$ and $\sigma_2^2(t)$ are the variances of the two segmented regions generated by thresholding at t, and C is a normalization constant. This measure is adapted from the work of Levine and Nazif [10]. According to this measure, a thresholding method is uniformly good if it selects a threshold such that each region is as uniform as possible.

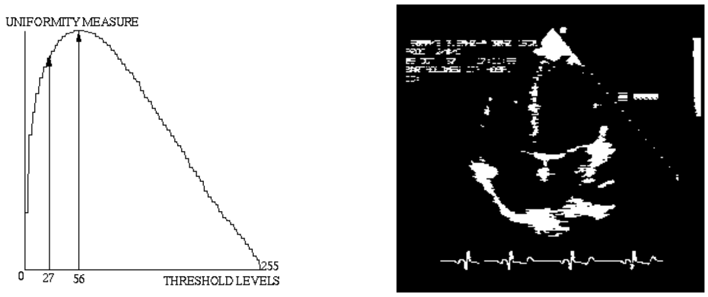

Figure 2: Evaluation of the uniformity measure for a two dimensional echocardiogram. Optimal global threshold is at 27 and optimal uniformity measure is at 56. The image is thresholded at threshold t=56.

Although this criterion evaluates the goodness of a threshold for the images with large uniform areas, it may fail to properly evaluate the goodness of the threshold for the images with nonuniform background or object regions. In Figure 2, we show a curve tracing the *uniformity measure* for all possible thresholds for the image displayed in Figure 1. The criterion is well behaved with a unique maxima, but the threshold selected at the maxima does not yield satisfactory segmentation. Although at this threshold the object pattern is detected and the regions have maximum uniformity, the shape and size of the pattern is not be preserved. The figure also shows that the better threshold of Figure 1, has a lower uniformity measure.

1.2 Shape criterion

To account for shape inaccuracies, Sahoo *et al*[9] suggest a *shape measure* for threshold evaluation. They assume a (3X3) neighborhood centered around the test pixel (x, y) with grey value $f(x, y)$, and define a general gradient $\Delta(x, y)$, as the root-mean-square vector sum of the grey level difference in all four directions. The shape measure $S(t)$ at threshold t is given by:

$$S(t) = \frac{\sum_{(} x, y)Sgn(f(x, y) - \overline{f_N(x, y)})\Delta(x, y)Sgn(f(x, y) - t)}{C} \tag{2}$$

where, $Sgn(x) = -1 or 1$ depending on whether or not x is negative, and $\overline{f_N(x, y)}$ is the average grey level of the neighborhood.

The shape measure expects a threshold such that all the points with positive gradient be above the threshold, and the points with negative gradient be below the threshold. The term *shape measure* seems to be a misnomer, because it depends mainly on the assumption that regions are uniform and the grey level gradients in the image correspond to the transitions between the two regions to be separated. Therefore, not

Figure 3: Evaluation of the shape measure for a two dimensional echocardiogram. Optimal global threshold is at 27 and optimal shape measure is at 46. The image is thresholded at threshold t=46.

surprisingly the optimal shape measure threshold generates the image regions similar to the ones generated by optimal uniformity measure threshold. In Figure 3, we show the variation of shape measure for a typical echocardiogram and the thresholded pattern generated by the optimal shape measure global threshold. The figure also shows that the global threshold with of Figure 1 has a lower shape measure.

Through the above study of uniformity and shape measures that evaluate the detection capability of a threshold, we observe that, a solution to the detection problem is not be sufficient for certain class of images. In this paper, we describe a method that adaptively propagates a precise local threshold over the entire image so that the precise pattern is extracted. This method facilitates extraction of the patterns from images whose object regions are not necessarily predominantly uniform. This method of extraction is advantageous to the fields such as medical image processing where direct measurements of the extracted pattern is of diagnostic interest, and to the fields that involve extraction of lines and strokes from digitized images of line drawings and text.

2 Image intensity map

In general, the intensity at a point in the image of an opaque surface depends on several parameters such as reflectance of the surface, brightness and directions of the light sources, distance of the surface from the image plane and the light source, and the direction of the surface normal with respect to light source and the camera aperture. If the object surface is opaque and is free from mirror like reflections, the brightness observed at a location does not change with change in the direction of observation[11]. Therefore the intensity at an image point can be approximated by:

$$I(x, y) = N_o + \int_{\Delta a} (\vec{I_o}(x', y') \cdot \vec{N}(x', y'))\rho(x', y')dx'dy' \tag{3}$$

where $\vec{I_o}(.)$ is the illumination over the incremental area Δa, with unit surface normal $\vec{N}(.)$, and N_o is the noise component, (x, y) and (x', y') are the corresponding coordinates in the image space and the object space. ρ is the object surface reflectance.

For document images, owing to relatively large source distances, and flat object surfaces, we approximate the above model by:

$$I(x, y) = N_o + \alpha I_o \int_{\Delta a} \rho(x', y')dx'dy' \tag{4}$$

where α is a constant, and I_o is the intensity magnitude.

The area Δa is finite in practice, thereby linearly smoothing the changes in the reflectance ρ. In a binary scene, reflectance ρ_o of the object region differs from the reflectance of the background ρ_b. Ideally, we should observe a contrast or grey level step transition of $I_o(\rho_o - \rho_b)$ at all the pattern edges. From equation 4, we observe that the imaging process linearly smoothes this change in reflectance to yield linearly smoothed image intensity gradients with slopes proportional to the ratio of local illumination to the resolution, $(I_o/\sqrt{\Delta a})$. If we approximate the incremental area Δa by a square of side δ, then the projection of the ramp in the image plane is δ(see Figure 5). A similar linear approximation model can obtained for B-scan ultrasound image data, where sound beam of finite area of cross section scans an internal organ, and reflected sound energy is registered in a two dimensional array [12]. This model of the data enables us to propagate a selected threshold at one location to the rest of the image by selecting the thresholds proportional to the local slopes of the object-to-background transition.

3 Selection of a regional threshold

The developed image intensity distribution map implies that in images of a binary scene, the object and background are separated by a linear ramp transition with slope proportional to the illumination. To *detect* the object pattern in these images, selecting a threshold anywhere on the ramp transition between the object and the background is sufficient. At different threshold levels we generate different pattern sizes. In

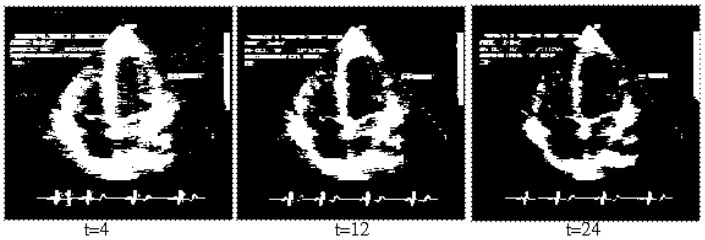

t=4 t=12 t=24

Thresholded patterns generated at different thresholds for an echocardiogram.

t=57 t=100 t=145

Thresholded patterns genearted at different thresholds for a digitized hand written address.

Figure 4: Pattern thickness is sensitive to the selected threshold. Both echocardiogram and a hand written text images show variation in pattern thickness with variation in threshold levels.

Figure 4, we show that the width of the generated pattern is sensitive to the selected threshold. The higher thresholds yield narrower patterns and missing regions, and the lower thresholds yield thicker patterns with extraneous regions. The selected threshold should be such that, it extracts the complete pattern of proper thickness, without misclassifying the extraneous regions. The proper positioning of the threshold is usually domain dependent. For example, for line extraction one would like to position the threshold so that a thin line is extracted, and for ultrasound heart images, the threshold should be at a level such that correct wall thickness is observed in the binarized pattern.

Although it is difficult to find a global threshold that meets the above requirements, often it is possible to use *a priori* knowledge of the domain to precisely select a regional threshold. For example, for line images or hand written or printed text images, we need to extract only thin line segments or strokes. Therefore we find a regional threshold by a binary search of the highest threshold that detects a line segment of specified length. For two dimensional echocardiograms, a cardiologist can point to a section of the wall with known thickness, and a regional threshold can be determined such that it generates a pattern of thickness close to the specified thickness[13].

4 Threshold Propagation

The main idea behind threshold propagation is to establish an invariant relation between a known regional threshold and the corresponding regional intensity gradient, and preserve this invariance over the entire image.

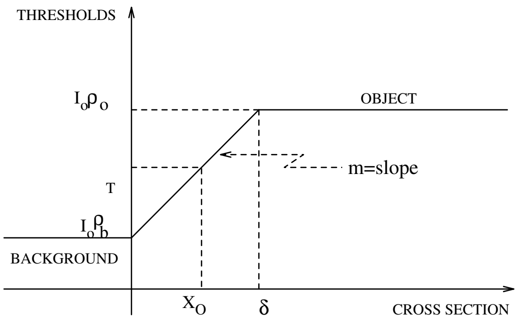

$$T = I_o \cdot \rho_b + m \cdot x_o \tag{5}$$

This gives the invariance:

$$\frac{T - I_o \cdot \rho_b}{m} = x_o \tag{6}$$

Figure 5: Cross section of the image pattern and the invariance relation.

To establish this invariance, let us study a perpendicular cross section of the image. Using the developed intensity map we schematically represent the cross section as shown in Figure 5.Let m be the slope of transition at any region, x_o be the precise boundary location. Then the correct regional threshold T is given by equation 5. Therefore by maintaining the *lhs* of the invariance equation 6, we propagate the threshold over the entire image that extracts the precise pattern.

4.1 Computation of the propagated threshold

Let t_{ref} be the selected regional threshold at a reference region, and T_{low} be the lowest global threshold that preserves the pattern generated by T_{ref} without misclassifying the background. Let $w_{low_{ref}}$ and w_{ref} be the widths of the pattern at the reference region, generated by thresholding at T_{low} and T_{ref} respectively. The widths are the thickness of the pattern measured perpendicular to the orientation of an elongated pattern. Therefore the slope of the intensity transition at the reference region is given by:

$$m_{ref} = \frac{2(T_{ref} - T_{low})}{(w_{low_{ref}} - w_{ref})} \tag{7}$$

$$\implies \quad \frac{2(T_{ref} - T_{low})}{m_{ref}} = w_{low_{ref}} - w_{ref} \tag{8}$$

This equation corresponds to the invariance relation given in equation 6, with intensity of the background region equal to T_{low}, and the invariance relation for any regional threshold T is:

$$w_{low_T} - w_T = w_{low_{ref}} - w_{ref} \tag{9}$$

Equation 9, indicates selecting a threshold at a cross section such that constant width difference of

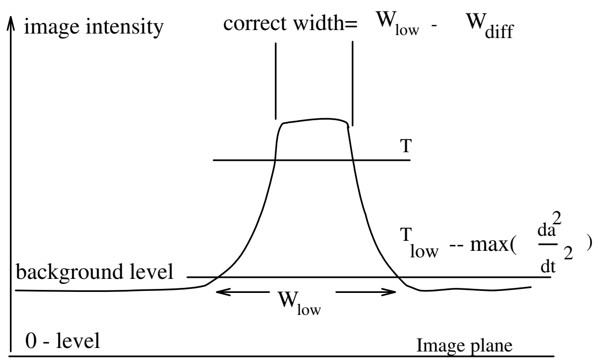

W_{low} = width at T_{low};
high = T_{max};
low = T_{low};
T = high;
While((high-low) $>$ 1) do{
    W_T = width at T;
    if($W_T > W_{low} - W_{diff}$)
        low = T;
    else
        high = T;
    endif
    T = (high + low)/2;
}

Figure 6: A binary search based threshold selection algorithm and a schematic of the adaptive threshold location (T) with respect to the global low threshold(T_{low}).

$w_{low_{ref}} - w_{ref}$ is maintained throughout the pattern. Without the knowledge of pattern orientation, it is difficult compute the widths. We have developed a method to efficiently compute a good approximation of pattern widths from the vertical and horizontal run lengths. For general line patterns with radius of curvature greater than 1.57 times the width, we show that the error in width estimation is less than 0.5%[14]. If w_v and w_h are the lengths of the vertical and horizontal runs passing through a point on the pattern, the width of the cross section w of the pattern at that point is given by:

$$w = \begin{cases} \min(w_v, w_h) & \text{if } \frac{\max(w_v, w_h)}{\min(w_v, w_h)} > 3.1 \\ \frac{1}{\sqrt{\frac{1}{w_v^2} + \frac{1}{w_h^2}}} & \text{otherwise} \end{cases} \tag{10}$$

Furthermore, the proposed width computation accounts for nearly horizontal and nearly vertical lines where horizontal and vertical runs do not intersect the line pattern. We compute the reference width difference w_{diff} as the difference between the average pattern widths at T_{ref} and T_{low}, at the reference section of the pattern. In Figure 6 we describe an efficient algorithm that uses binary search to select a local threshold that maintains the width difference. The figure also shows a schematic diagram of the threshold locations. This method is efficient, and yields promising results. The propagated local threshold T is computed at all points on the image, and all pixels with intensities higher than T are classified as the pattern pixels. At the points on the background where no pattern is detected by T_{low}, we set threshold $T = T_{ref}$. In addition, we morphologically vary the threshold using the idea developed in [15] to obtain smooth continuous patterns.

4.2 Computation of the global low threshold

To determine the low threshold T_{low} we scan through the binary patterns of the image generated by a series of decreasing threshold levels, starting from the reference threshold T_{ref}. Consistent with our assumed model of the image, the area increases with decrease in the selected threshold. The level at which the threshold starts classifying the background regions as the object, the area abruptly increases. At that point, we select the previous level as the low global threshold. This method can be implemented efficiently through simple histogram analysis.

Let $H[i]_0^{T_{max}}$ be the histogram of the entire image. Then the area a_t of the thresholded pattern at any threshold t is given by:

$$a_t = \sum_{i=t}^{T_{max}} H[i] \tag{11}$$

and the rate of change of the area is given by:

$$\frac{da}{dt}|_t = (a_t - a_{t+1}) = H[t]$$

$$\Longrightarrow \frac{da^2}{dt^2}|_t = H[t] - H[t+1] \tag{12}$$

The level at which there is abrupt change in area increase, the magnitude of $\frac{da^2}{dt^2}$ is maximum. Therefore we define the low global threshold T_{low} as the highest intensity level at which the abrupt change is observed.

$$T_{low} = \max_i \ni \{\forall t, j < T_{ref} \left|\frac{da^2}{dt^2}\right|_{t=i} \geq \left|\frac{da^2}{dt^2}\right|_{t=j} \} \tag{13}$$

Because of noise, and scaling used in imaging instruments, this method of threshold computation may yield a wrong low threshold. For example, if the image is histogram equalized or scaled, it may have no pixels in some grey levels. This may result in detection of T_{low} at one of such valleys. We can improve the robustness by smoothing the histogram. We simulate the histogram smoothing by tracking the regional maxima of the histogram for computing $\frac{da^2}{dt^2}$.

$$\frac{da^2}{dt^2}|_t = H[t] - \max_{i=t+1}^{T_{ref}} H[i] \tag{14}$$

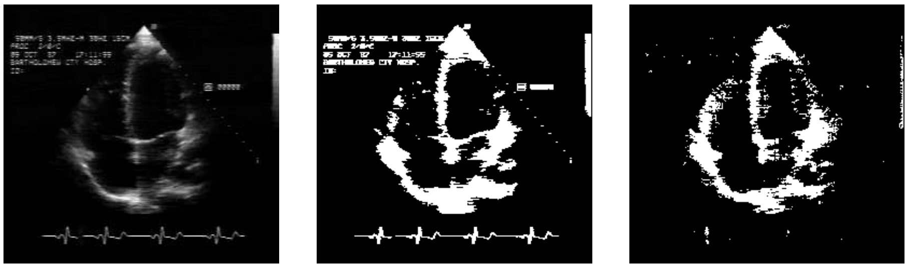

Figure 7: Two dimensional echocardiograms of Figure 1 (left and center), with adaptively thresholded image in the right.

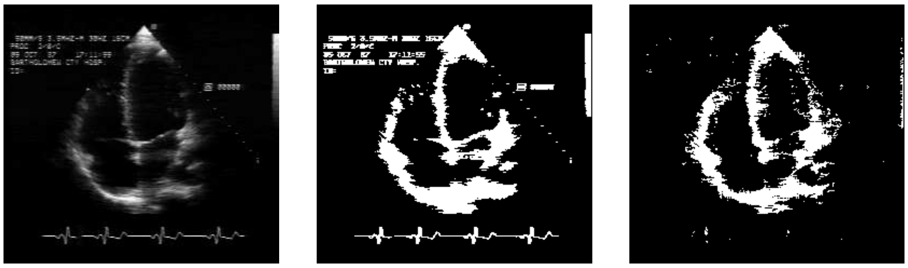

Figure 8: A two dimensional echocardiogram (left) thresholded by $T_{ref} = 27$ without adaptation (center) and with adaptation (right).

5 Results

In Figure 7, we compare the outputs generated by our algorithm with and without adaptative propagation. The image in the center was generated by the threshold T_{ref} maintained constant throughout the image. This image has the threshold that detects the patterns of correct width for the most part, but it has missed some wall sections. In the right image, this threshold was adapted by maintaining the constant W_{diff} over the entire image, and so the walls are detected even in the barely visible sections of the original image. Thresholding of a second echocardiogram frame is shown in Figure 8.

This method works well on optical images of hand written text. In Figure 9 we compare the thresholding with and without adaptive propagation. The original image in the top row is a digitized image obtained from a USPS mail piece. The image in the center row is the patterns generated by the global threshold T_{ref} selected such that it detects narrow line patterns. In the bottom row we show the output generated by our adaptive propagation method. It clearly generates connected uniform patterns. A second example of processing on an optical image is shown in Figure 10[2]. Clearly the adaptive thresholding method extracts

[2]For this example $T_{low}$is found by a varient of the current method, that accounts for nonuniform backgrounds.

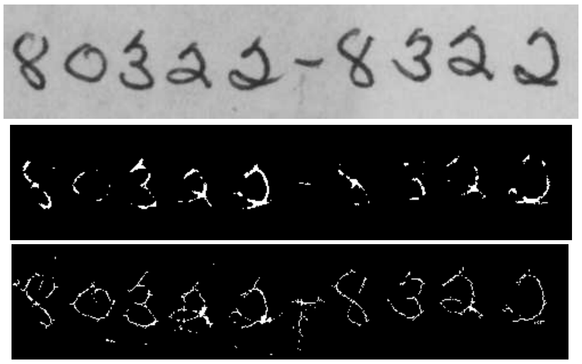

Figure 9: The top image is the grey tone image obtained from a USPS mail piece. The middle image is the binary pattern generated by the global threshold T_{ref} and the bottom image is the binary pattern generated by adaptive propagation of the threshold.

Figure 10: Optical image of a hand drawn line sketch(left), was thresholded by the global threshold T_{ref} selected so that thin line is detected. The right image is the output by adaptive propagation of T_{ref}.

narrow continuous line patterns.

To visualize the adaptation of the threshold, in Figure 11, we show a three dimensional rendering of the threshold values at all the image points. The threshold varies such that wall sections are detected even in the barely visible areas.

6 Conclusions

We have described a new method for pattern extraction by adaptive propagation of a known regional threshold. We approximate the imaging process by a linear model that shows that slope of the grey level transitions is proportional to the illumination intensity in optical images or gain compensation in ultrasound images. The known regional threshold is then propagated over the entire image or the image sequence in case of a dynamic scene, such that the ratio of threshold to slope is maintained constant. We show the outputs generated by this algorithm for both echocardiograms and optical images of hand written text. This

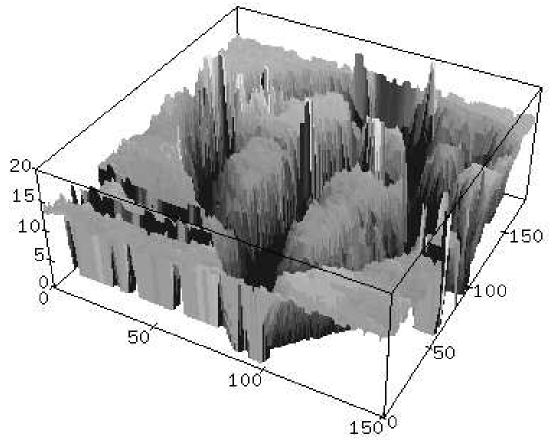

Figure 11: Threshold map generated by the adaptively propagated threshold for the second image shown in Figure 8.

method should be useful in the fields such as medical image processing where direct measurements of the extracted pattern is of diagnostic interest, and to the fields that desire extraction of thin continuous lines and strokes from digitized images of line drawings and text.

References

[1] David Sher, Shriram Revankar, and Steven Rosenthal. Computer methods in quantitation of cardiac wall parameters from two dimensional echocardiograms: A survey. *International Journal of Cardiac Imaging*, 1992 (to appear).

[2] R.W. Smith. Computer processing of line images: a survey. *Pattern Recognition*, 20(1):7–15, 1987.

[3] J.R. Ullman. Binarization using associative addressing. *Pattern recognition*, 6:127–135, 1974.

[4] Shriram Revankar and David B. Sher. Morphologically influenced adaptive threshold to extract myocardium from a sequence of two-dimensional echocardiograms. In *Proceedings: Fifth Annual Graduate Conference in Computer Science, State University of New York at Buffalo*, pages 31–41, March 23 1990.

[5] C.K. Chow and T. Kaneko. Boundary detection of radiographic images by a threshold method. In *Proceedings IFIP Congress - 71, Booklet - TA-7*, pages 130–134, North Holland, Amsterdam, 1972.

[6] R.N. Wolfe. A dynamic thresholding technique for quantization of scanned images in automatic pattern recognition. *National Security Industrial Association, Washington D.C.*, pages 143–162, May 1979.

[7] H.Ogawa and K. Taniguchi. Thinning and stroke segmentation for hand written chineses character recognition. *Pattern recognition*, 15(4):298–308, 1982.

[8] J.S. Weszka and A. Rosenfeld. Threshold evaluation techniques. *IEEE Transactions on System Man and Cybernetics*, SMC-8:622–629, 1978.

[9] P.K. Sahoo, S. Soltani, and A.K.C Wong. A survey of thresholding techniques. *Computer Vision, Graphics and Image Processing*, 41:233–260, 1988.

[10] M.D. Levine and A.M. Nazif. Dynamic measurement of computer generated image segmentation. *IEEE Transactions on Pattern Recognition and Machine Intelligence*, PAMI-7:652–655, 1985.

[11] Brthold K.P. Horn. Understanding image intensities. *Artificial Intelligence*, 8:201–231, 1977.

[12] James F. Havlice and Jon C. Taenzer. Medical ultrasonic imaging: An overview of principles and instrumentation. *Proceedings of the IEEE*, 67(4):620–641, April 1979.

[13] Shriram Revankar and David Sher. Maximal detection of myocardium in echocardiograms for supervised refinement. In *Proceedings of the IEEE Eighteenth Annual Northeast Bioengineering Conference*, March, 13-14 1992.

[14] Shriram Revankar and David Sher. Supervised binarization of echocardiograms by adaptive thresholding. Technical Report 92-11, Department of Computer Science, SUNY at Buffalo, 1992.

[15] Shriram Revankar. Computer drafting of hand drawn line sketches. Master's thesis, Department of Computer Science and Engineering, Indian Institute of Technology, Madras, India, August 1987.